Available online at www.sciencedirect.com

jmr&t Journal of Materials Research and Technology

www.jmrt.com.br

Original Article

Clay/chitosan biocomposite systems as novel green carriers for covalent immobilization of food enzymes

Ilaria Cacciotti[a], *Claudio Lombardelli*[b], *Ilaria Benucci*[b,*], *Marco Esti*[b]

[a] *Department of Engineering, University of Rome "Niccolo Cusano", Via Don Carlo Gnocchi 3, 00166 Rome, Italy*

[b] *Department of Agriculture and Forestry Science (DAFNE), Tuscia University, Via S. Camillo de Lellis snc, 01100 Viterbo, Italy*

ARTICLE INFO

Article history:
Received 3 January 2019
Accepted 2 June 2019
Available online 15 June 2019

Keywords:
Clay
Chitosan
Food enzymes
Microstructure
Kinetic parameters.

ABSTRACT

In this work, innovative green composite systems, based on high amounts of montmorrilonite (MMT) and low amounts of chitosan in different relative ratios (70:30, 75:25, 80:20, % w/w), were proposed as potential alternatives to the free nanoclay particles, commonly used as carriers for enzymes covalent immobilization. In details, two different MMT were selected, i.e. SMP (a high purity unmodified MMT) and Optigel (OPT, an activated food-grade MMT). The chitosan was used both to make the clays appropriate supports for the enzymes covalent binding, and to maintain the clay particles together in a unique structure, acting as a binder. The mechanical, thermal, and chemical properties of the obtained composite systems were studied. Moreover, the catalytic properties of a protease covalently immobilized on these carriers were investigated in a model wine-like medium toward a synthetic substrate. OPT based composite systems presented higher σ_{max} and Young modulus values with respect to the SMP based ones, due to OPT better distribution and interaction with the chitosan. Irrespective of nanoclays amount, SMP and OPT composite systems appeared suitable carriers for the covalent immobilization of protease, with an immobilization yield of 18% and 14–17%, respectively. The highest product release velocity was detected when the protease was immobilized on OPT carriers (V_{max} 10.49-10.74 mIU mg$^{-1}_{IP}$), and the greatest apparent affinity when it was linked to SMP composite systems (K_a 2.19–3.10 min^{-1} μM).

1. Introduction

In recent years, clay minerals have been applied as attractive inorganic supports for enzyme immobilization [1], due to their low cost, chemical inertia, thermal stability, well-defined layered structure and ion-exchange ability [2]. Clay minerals, and smectites in particular, are characterized by high

* *Corresponding author.*
E-mail: ilaria.be@unitus.it (I. Benucci).

https://doi.org/10.1016/j.jmrt.2019.06.002

protein adsorption affinity due to the presence of exchangeable cations (i.e. Na^+ or Ca^{2+}) in the interlayer space. These cations can be replaced by positively-charged enzyme molecules through a cation exchange reaction [1].

For this reason, various authors have used Na-montmorillonite (Na-MMT) and Ca-montmorillonite (Ca-MMT) for the covalent and physical immobilization of enzyme molecules, such as catalase [3], glucoamylase [4], α-amylase [5], lipase [6], laccase [7] and invertase [8]. Despite non-covalent adsorption onto clay minerals be simple and cost effective immobilization technique, its main criticism is the limited stability of adsorbed enzymes, due to the weak interactions between enzyme and support, as well as to the environmental conditions, i.e. pH, temperature, ionic strength and biomolecule concentration [9].

The structural and chemical characteristics of layered clay minerals could be easily improved by the addition of organic and polymeric biomolecules. Among them, chitosan (CS) can be used to supply additional functional groups (i.e. hydroxyl and amino groups), in order to render the clays suitable supports for the covalent binding of enzymes. In this regard, α-amylase, β-amylase, glucoamylase and β-glucosidase have been covalently immobilized on clay/CS composites, showing an improved stability when applied at acidic pH [10,11].

Clay/CS composite membranes have been also investigated for application in pharmaceutical industry as controlled drug-delivery vehicles [12,13], and in food industry as packaging materials [14–16]. One of the first attempts to form an organo-mineral complex involving CS was carried out by Clapp and Emerson [17]. For this purpose, they used homoionic smectites (Ca-MMT) and found that the positively charged CS was adsorbed at the same extent as the most strongly adsorbed neutral species. The mechanisms that control smectite–biopolymer interactions depend on the nature of both the involved biopolymers and the clay mineral hosts. Given that diluted acid solutions are required to dissolve CS, this biopolymer behaves in solution as a positively charged polyelectrolyte, being able to intercalate MMT and other smectites by ion-exchange reactions [18]. The intercalation mechanism is mainly driven by electrostatic interaction of the positively charged amino groups of CS chains with the negatively charged sites in the clay mineral layers. Besides, hydrogen bonding and other types of interaction may contribute to the adsorption mechanism. As proved by Darder et al. [19] when the starting amount of CS is lower than the cationic exchange capacity of the clay, the intercalation of CS in MMT takes place in monolayer configuration.

In the present work SMP (a high purity unmodified MMT) and Optigel (OPT, an activated MMT) were selected, on the basis of previous results related to the production of CS nanocomposite films loaded with different kinds of nanoclays (organomodified MMT, bentonite and sepiolite) in low concentration (1–5% wt) [20]. Indeed, among the tested nanoclays, SMP allowed to improve the mechanical properties of CS based films, whereas OPT appeared interesting as food-grade material, since it is the only nanoclay authorized to be used in contact with food. Thus, the novelty and significance of this paper consist in combining the selected MMT powders with low amounts of chitosan, in different relative ratios (MMT:CS 70:30, 75:25 and 80:20, % w/w), providing novel green carriers for the immobilization of food enzymes. Indeed, the chitosan addition allowed to make the clays appropriate supports for the covalent binding of enzymes, providing them with additional functional groups (i.e. hydroxyl and amino groups), and to maintain the clay particles together in a unique structure, acting as a binder. The obtained compact novel clay/CS composite systems were able to provide a favorable microenvironment for the enzyme molecules and allowing them the retention of catalytic activity [21,22].

The aim of the present study was to evaluate the potential application of the obtained clay/CS systems as novel carriers for enzyme covalent immobilization. The mechanical, thermal and chemical properties of the produced composite systems, as well as the catalytic properties of a proteolytic enzyme (bromelain from pineapple stem) covalently immobilized on these carriers, were investigated. Finally, biocatalysts were tested in model wine like medium toward a synthetic substrate.

2. Materials and methods

2.1. *Materials*

Shellfish derived chitosan (CS) powder (low molecular weight 50–190 kDa; percentage of deacetylation 75%), pineapple stem bromelain (BR, EC 3.4.22.32), glycerol (≥99.5%), glutaraldehyde (GDH, 25% v/v) were purchased from Sigma-Aldrich (Milan, Italy). Two different nanoclays, i.e. high purity unmodified montmorillonite (SMP) and activated food-grade montmorillonite (Optigel, OPT), were kindly provided by Zhejiang Fenghong New Material Co., Ltd (China) and BYK Additives GmbH (Germany), respectively. The selected tripeptide chromogenic substrate, i.e. Bz-Phe-Val-Arg-p-nitroaniline (pNA), was purchased from Bachem (Germany).

2.2. *Preparation of clay/CS composite systems by solvent casting*

Composite systems were obtained by solvent casting method, using low molecular weight CS powder blended with glycerol in the weight ratio CS:glycerol 75:25, as described in literature [20,23]. Two different nanoclay types, SMP and OPT, were tested, in various w/w percentages with respect to the chitosan (i.e. 70, 75 and 80% w/w), obtaining three different compositions for each clay. Firstly, various amounts of nanoclays were ultrasonicated in aqueous solution (Ultrasonicator Sonics Vibracell CV33, 750 W, 20 kHz, amplitude 30%, time 30 min) and then the proper contents of acetic acid (2% v/v), low molecular weight CS and glycerol were added; the obtained suspensions were magnetically stirred overnight. The CS solutions were laid down onto plastic Petri dishes, placed in a fume hood at room temperature for 48 h to complete the solvent evaporation and the composite system formation. Furthermore, as a reference, a system composed of only CS and glycerol was produced following the same procedure. The obtained samples were designed as Clay-free for the CS/glycerol based film and SMP-*x* and OPT-*x* in the case of clay-loaded composites (where *x* is the percentage w/w of the used nanoclay).

2.3. Characterization of clay/CS composite systems

To identify the functional groups of the produced samples, Fourier Transform Infrared (FT-IR) spectra were acquired by means of a FT-IR spectrometer (Jasco, FT/-6600) equipped with an attenuated total reflectance (ATR), in the following conditions: wavenumber range 600–4000 cm^{-1}, spectral resolution 4 cm^{-1} and scans number 32.

The morphology of the obtained supports was investigated by Field-Emission Gun Scanning Electron Microscope (FEG-SEM, Cambridge Leo Supra 35, Carl Zeiss). The thermal properties of the prepared systems were studied by differential scanning calorimetry (DSC, TAInstruments Q2000) measurements that were performed under the following conditions: sample weight ~5 mg, nitrogen atmosphere (N_2 flow rate 50 cm^3 min^{-1}), range temperature 25–400 °C, heating rate 10 °C min^{-1}. Uniaxial tensile tests were performed on dog-bone specimens (width 4.8 mm, length 22.25 mm), following the ASTM D1708 and ASTM D882 standards, at 1.2 mm min^{-1}, by an electromechanical apparatus equipped with a 50 N load cell (Lloyd LRX Lloyd Instruments). Eight specimens were tested for each sample. All mechanical properties were calculated considering the nominal specimen cross-section.

2.4. Enzyme covalent immobilization on clay/CS composite systems

Before the immobilization, clay/CS composite systems were neutralized by shaking overnight in 26% (v/v) ethanol–NaOH 2 M solution, in order to render them water insoluble [24]. Membranes were then cut into squares (10 mm × 10 mm) with a razor blade. The immobilization procedure was performed activating the surface of each clay/CS composite system square with 1 mL of GDH (3% v/v), used as cross-linker. The suspension was kept under constant agitation for 2 h at room temperature, and then profusely washed with distilled water. Thereafter, 1 mL of stem BR preparation (2.2 mg protein mL^{-1}), previously solubilized in the immobilization buffer (tartaric acid/sodium tartrate 0.03 M, pH 3.2), was added to the activated clay/CS composite system square, shaking it (150 rpm, at 20 °C) overnight.

The applied immobilization procedure is based on the use of chitosan (as carrier) containing amino groups in its structure, and GDH (as cross-linker), which reacts with the amino group of chitosan to form a Schiff base. Thereafter, the covalent linkage occurs between the activated carrier and the amino groups of Lys residues in the enzyme structure [25].

At the end of the incubation time, samples were washed three times with immobilization buffer and then left to stand for 20 min in a 0.1 M glycine solution. At the end of the immobilization procedure, biocatalysts were washed three times with 2 M NaCl solution to remove all non-covalently bound proteins and the composite systems were resuspended in the immobilization buffer. All supernatants were collected and diluted with buffer solution to a constant final volume to determine the bound protein. The immobilization yield (IY, %) was determined by Bradford's method [26], using Coomassie brilliant blue reagent and measuring absorbance at 595 nm. Bovine serum albumin (BSA) was used as standard. The percentage of bound protein was indirectly determined as the difference between the amount of protein in solution before and after immobilization.

2.5. Enzymatic activity determination

Proteolytic activity toward the selected substrate (Bz-Phe-Val-Arg-pNA) was tested in wine-like acidic medium, designated as model wine, which was a 0.03 M tartaric acid/sodium tartrate solution, pH 3.2, containing ethanol (12% v/v). Protease activity was determined measuring the cleavage of the substrate, resulting in free pNA release, which was spectrophotometrically (UV-visible spectrophotometer, Shimadzu UV, Milan, Italy) detected evaluating the change in absorbance (at 410 nm) vs time for 10 min. Specific activity, calculated in mIU of pNA produced ε mM$\equiv$8.480 mM^{-1} cm^{-1} for pNA [27], was expressed as mIU mg^{-1} of immobilized protein (mIU $mg^{-1}{}_{IP}$). A blank correction was made using a sample that did not contain enzyme. All measurements were performed in triplicate.

2.6. Kinetic study of immobilized protease

A kinetic study of pineapple stem bromelain immobilized on clay/CS composite systems, by means of GDH cross-linking, was carried out in model wine, fortified with Bz-Phe-Val-Arg-pNA substrate (0–750 μM).

Kinetic parameters (K_M, k_{cat} and $K_a = k_{cat}/K_M$) were determined according to Michaelis–Menten equation, fitting experimental data by a non-linear regression procedure (GraphPad Prism 5.01, GraphPad software, Inc.). The goodness of-fit of each data set to its best-fit theoretical kinetic curve was assessed as the square of the correlation coefficient (R^2).

V_{max} represents the maximum velocity at which enzyme catalyzes the reaction, K_M (Michaelis–Menten constant) is equal to the substrate concentration when the initial velocity is one-half of the V_{max}, indicating the catalysis efficiency. k_{cat} (turnover number) relates to the number of substrate molecules converted into product, in a unit of time, by an enzyme molecule. Moreover, affinity constant ($K_a = k_{cat}/K_M$) reflects the affinity of the enzyme toward substrate, and it refers on both reaction steps and expresses the overall catalytic efficiency.

2.7. Statistical analysis

Data were analyzed by one-way completely randomized Analysis of Variance (ANOVA) with the EXCEL® Add-in macro DSAASTAT, followed by Tukey Honestly Significant Difference (Tukey HSD) post hoc test (P = 0.05) for multiple comparisons of samples.

3. Results and discussion

3.1. Microstructural, thermal and mechanical properties of chitosan/clay systems

The morphology of the produced systems was investigated by means of FESEM analysis. It is interesting to note that all systems based on OPT were characterized by a very uniform

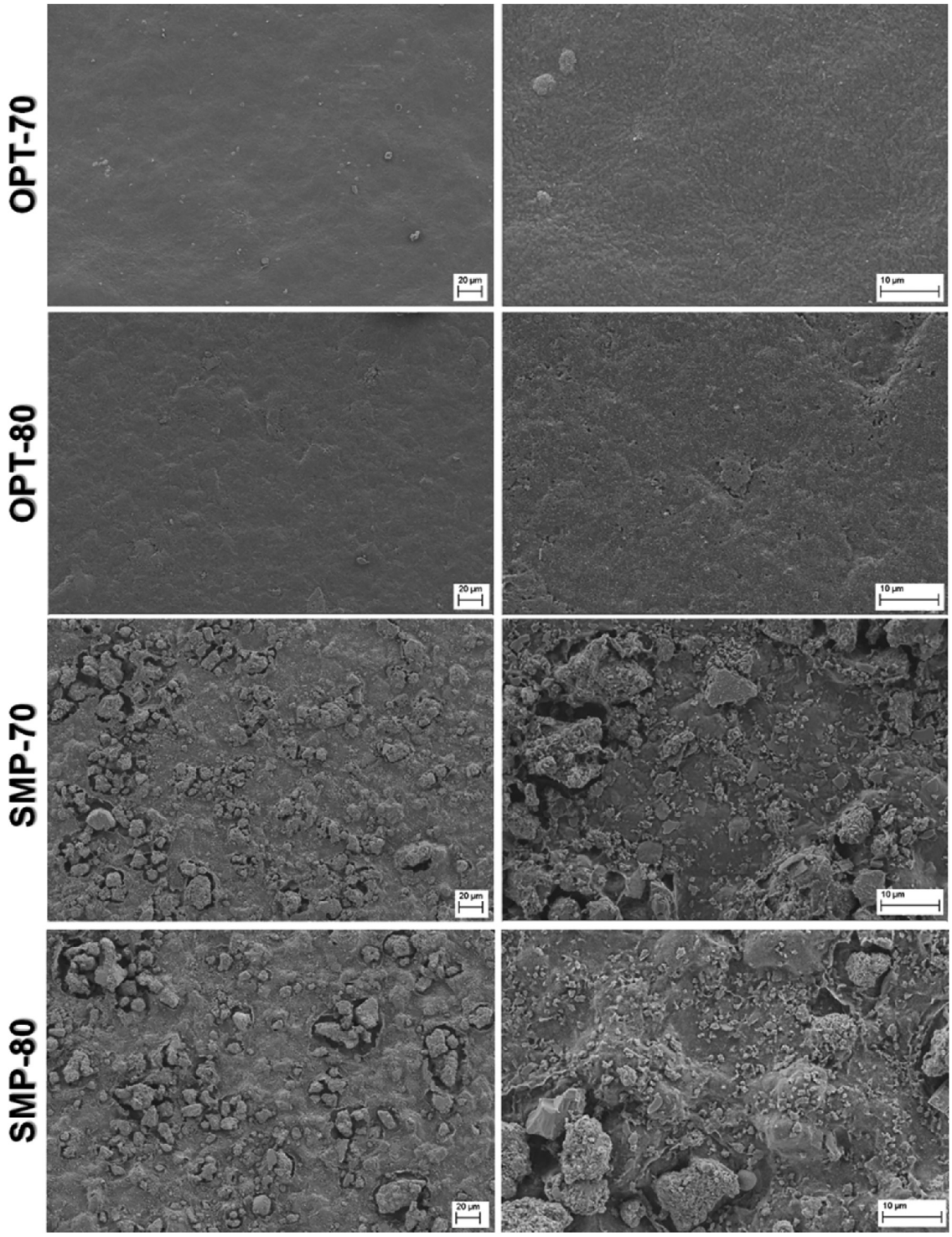

Fig. 1 – FE-SEM micrographs of the plane view surfaces of OPT-70, OPT-80, SMP-70 and SMP-80 systems.

and homogeneous surface, whereas the SMP addition led to the presence of several agglomerates and defects (Fig. 1). The occurred immobilization of bromelain on the surface of the produced films was confirmed by observation at SEM. As an example, in Fig. 2, the SEM micrographs of SMP-70 and OPT-70, before and after the enzyme immobilization, are compared, evidencing the presence of a continuous and uniform organic layer on the film surface, ascribable to the enzyme immobilization.

In order to investigate the possible CS/clays interaction, FTIR/ATR spectra were acquired on all produced systems. In Fig. 3 the ATR spectra of the clay-free film and of films loaded with 80% clays are compared, revealing the typical chitosan vibration modes [28] in all cases. In addition, the clay loaded

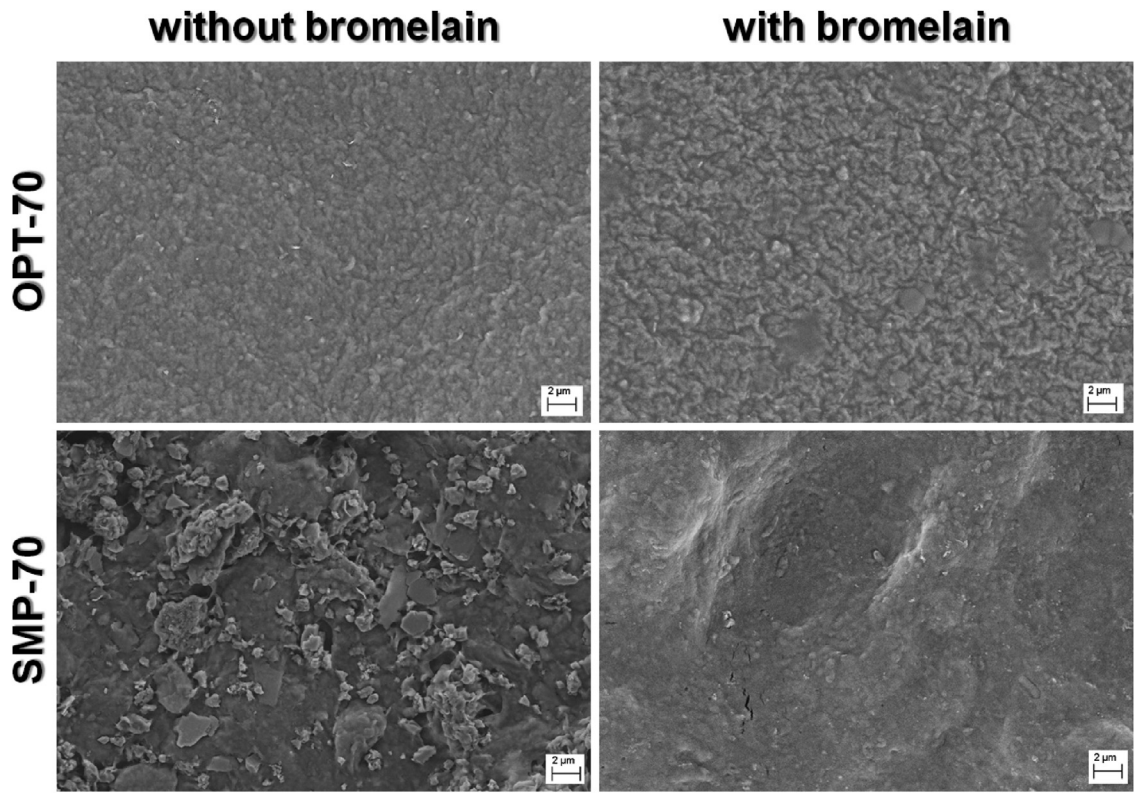

Fig. 2 – FE-SEM micrographs of the plane view surfaces of OPT-70 and SMP-70 systems before and after bromelain immobilization.

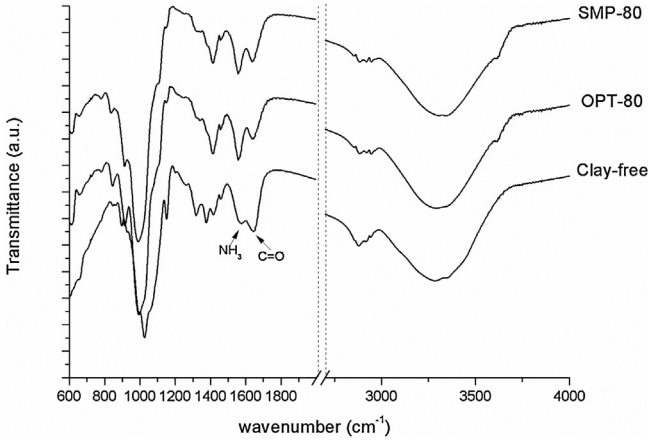

Fig. 3 – FTIR/ATR spectra of clay-free, OPT-80 and SMP-80 systems.

films spectra reveal the typical vibrational modes of clays, including the characteristic absorption bands at ~3622 cm^{-1} (νOH,e stretching vibration of AlOH and SiOH), ~3416 cm^{-1} (νOH, stretching vibration of H_2O), ~1628 cm^{-1} (δHOH, bending vibration of H_2O), ~1118 cm^{-1} and at ~980 cm^{-1} (νSi—O, stretching vibration of SiO), ~912 cm^{-1} (δAl—Al—OH, bending vibration of AlAlOH), ~843 cm^{-1} (δAl—Mg—OH, bending vibration of AlMgOH) [29,30].

The occurred electrostatic interaction between the chitosan NH_3^+ groups and the negatively charged sites of the clay [19] was corroborated by the identification of a slight shift of the peaks at 1574 cm^{-1} toward a lower frequency (around 1554 cm^{-1}), in agreement with Silva et al. [31]. Indeed, this peak is ascribed to the vibrational modes of chitosan protonated amine group (δ_{NH_3}) [19] and its shift toward lower wavenumbers is an indication of the ionic exchange between chitosan and montmorillonite and, thus, of the intercalation of chitosan within the montmorillonite structure. The secondary amide band (ν1) at 1645 cm^{-1} of chitosan is overlapped with the δHOH bending vibration band at 1628 cm^{-1} of the water molecules associated with the chitosan/clay films, which are present as in the starting clay, as expected for a biopolymer with high water retention capability [32,33]. Comparing the spectra of SMP and OPT based samples, it is possible to conclude that the interaction of the chitosan with both clays (SMP and OPT) is similar, as expected, due to the comparable chemical composition.

Furthermore, the influence of the nanoclay fillers on the chitosan thermal properties was investigated by means of DSC measurements. In Fig. 4 the DSC first heating run curves of all the chitosan based systems were compared. In most samples a broad endothermic peak was observed at approximately 105–120 °C (Table 1), caused by the dissociation process of interchain hydrogen bonding of CS (T_{IHB}) [34], as well as an exothermic band at approximately 285–315 °C ascribed to CS decomposition [35–37]. It is interesting to note that the nanoclays based systems were characterized by a decreased hydrogen bonds dissociation temperature value with respect to the clay-free sample (121 °C), as well as a decrement of the related enthalpies, particularly for SMP based samples. As regards to chitosan degradation temperature (T_d), remarkably

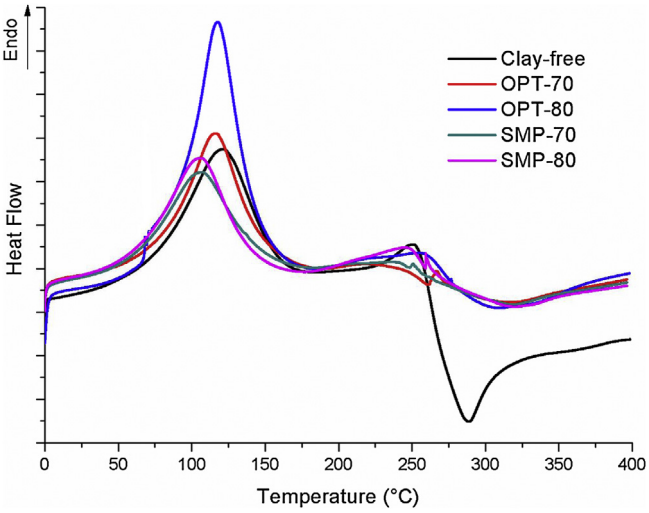

Fig. 4 – DSC first heating curves of clay-free, OPT-70, OPT-80, SMP-70 and SMP-80 systems.

Table 1 – Thermal properties of clay-free, OPT-70, OPT-80, SMP-70 and SMP-80 samples, related to the DSC first heating scan.

Sample	T_{IHB} (°C)	ΔH_{mI} (J/g)	T_d
Clay-free	121	259	287
OPT-70	116	331	311
OPT-80	118	442	306
SMP-70	107	259	316
SMP-80	106	293	313

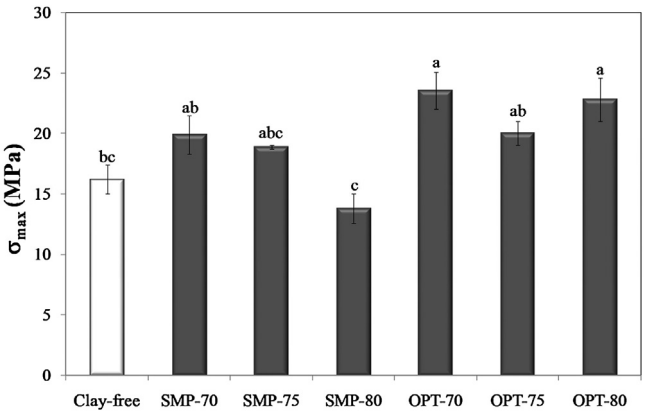

Fig. 5 – Ultimate tensile stress (σ_{max}) of clay/CS composite systems obtained from chitosan films added with ultrasonicated clays at high contents (70, 75 and 80% (w/w) with respect to the chitosan). The clay-free chitosan carrier is reported as reference. Reported values are mean ± 95% confidence interval of triplicate measurements. The used roman letters (i.e. a, b, c, ab, bc and abc) indicate significant differences (Tukey's test, $P < 0.05$) in the mechanical results among the investigated samples.

enhanced temperature values were detected for the composite systems compared to the clay-free sample (287 °C), demonstrating that the nanoclays are able to act as thermal barrier, as expected.

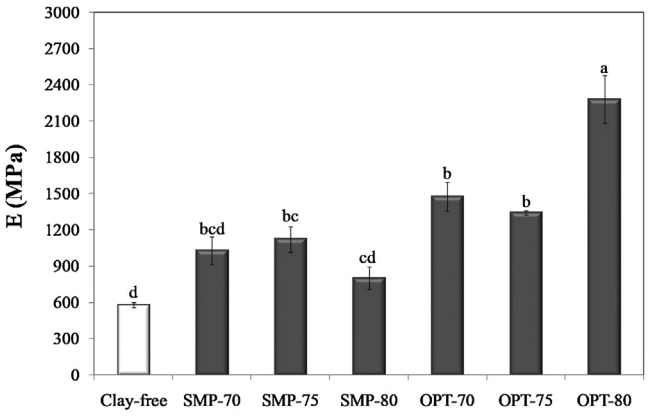

Fig. 6 – Tensile modulus (E) of clay/CS composite systems obtained from chitosan films added with ultrasonicated clays at high contents (70, 75 and 80% (w/w) with respect to the chitosan). The clay-free chitosan carrier is reported as reference. Reported values are mean ± 95% confidence interval of triplicate measurements. The used roman letters (i.e. a, b, d, bc, cd and bcd) indicate significant differences (Tukey's test, $P < 0.05$) in the mechanical results among the investigated samples.

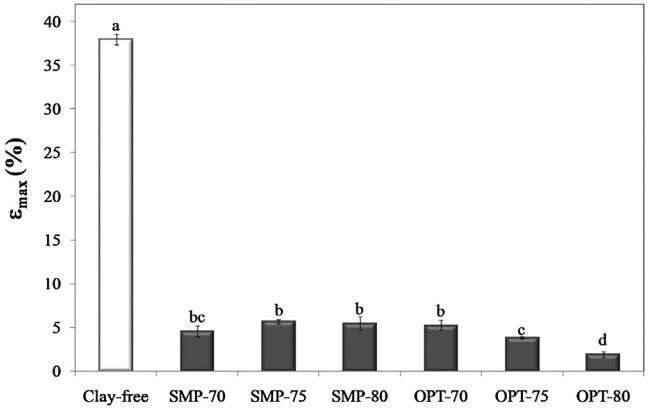

Fig. 7 – Elongation at break (ε_{max}) of clay/CS composite systems obtained from chitosan films added with ultrasonicated clays at high contents (70, 75 and 80% (w/w) with respect to the chitosan). The clay-free chitosan carrier is reported as reference. Reported values are mean ± 95% confidence interval of triplicate measurements. The used roman letters (i.e. a, b, c, d, and bc) indicate significant differences (Tukey's test, $P < 0.05$) in the mechanical results among the investigated samples.

To analyze the mechanical properties of the obtained systems, uniaxial tensile tests were performed (Figs. 5–7). Higher σ_{max} values were detected in the case of OPT based composite systems with respect to the SMP based ones (Fig. 5), due to its better distribution and interaction with the chitosan chains, as evident from the reported SEM micrographs (Fig. 1). Furthermore, in the case of OPT samples the σ_{max} values were comparable independently of the OPT amounts, whereas in the case of SMP composites a decrement was observed with the increasing SMP percentage, due to the increment of the agglomerates. Similarly, Young modulus (E) appeared to be

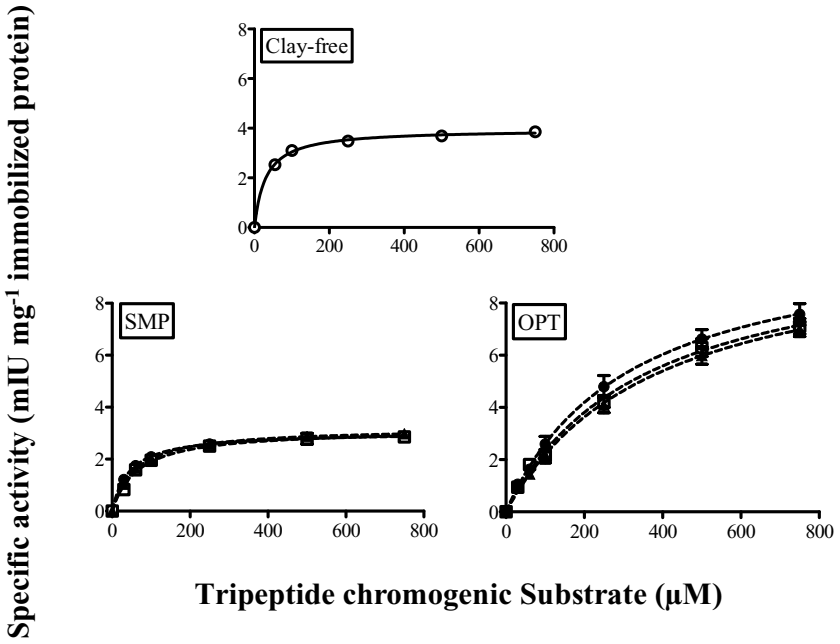

Fig. 8 – Kinetic curves of bromelain immobilized on clay/CS composite systems loaded with different nanoclays (SMP or OPT) at various concentrations: 70 (●), 75 (□) and 80 (▲) % w/w. Bromelain covalently linked on the clay-free chitosan carrier is reported as reference. Proteolytic activity was determined toward Bz-Phe-Val-Arg-pNA substrate (0–750 μM), in model wine (tartaric acid/sodium tartrate solution 0.03 M, pH 3.2, containing 12% v/v of ethanol at 20 °C).

Table 2 – Immobilization yield (IY), maximum velocity (V_{max}), Michaelis–Menten constant (K_M), turnover number (k_{cat}) and affinity constant (K_a) of bromelain, immobilized on clay/CS composite systems loaded with different nanoclays (SMP or OPT) at various concentrations: 70, 75 and 80% w/w. Bromelain covalently linked on the clay-free chitosan carrier is reported as reference. Kinetic parameters were determined toward Bz-Phe-Val-Arg-pNA substrate (0–750 μM), in model wine (tartaric acid/sodium tartrate solution 0.03 M, pH 3.2, containing 12% v/v of ethanol at 20 °C). Immobilized enzyme parameters are mean of triplicate measurements.

Sample	IY (%)	V_{max} (mIU mg$^{-1}_{IP}$)	K_M (μM)	k_{cat} (min^{-1})	K_a (min^{-1} μM)	R^2
Clay-free	23^{a}	3.91^{b}	28.70^{b}	139.00^{f}	4.90^{a}	0.99
SMP-70	18^{bc}	3.05^{b}	45.01^{b}	139.71^{f}	3.10^{b}	0.97
SMP-75	18^{b}	3.15^{b}	65.75^{b}	144.15^{e}	2.19^{cd}	0.96
SMP-80	18^{bc}	3.21^{b}	59.95^{b}	147.04^{d}	2.45^{bc}	0.98
OPT-70	15^{c}	10.74^{a}	312.70^{a}	555.84^{b}	1.78^{cde}	0.98
OPT-75	14^{c}	10.50^{a}	351.60^{a}	572.27^{a}	1.63^{de}	0.98
OPT-80	17^{bc}	10.49^{a}	378.00^{a}	495.15^{c}	1.31^{e}	0.98

For each parameter, values with different roman letters are significantly different (Tukey's test, $P < 0.05$).

remarkably improved in the case of OPT based systems particularly for OPT-80 (Fig. 6). Consequently, a significant decrease in elongation at break was observed (Fig. 7), due to the presence of an inorganic component in very high concentration.

Based on the collected mechanical data (Figs. 5–7) and SEM micrographs of the sample surfaces (Fig. 1), it is possible to conclude that the used chitosan is able to act as binder and to entrap the dispersed inorganic nanoparticles, obtaining compact films. Moreover, the better mechanical behavior of OPT based composites could be ascribed to the higher compatibility between the used nanoclays and the chitosan, as corroborated by DSC data (Table 1), and by the different morphology and agglomeration tendency of the considered nanoclays. Indeed, both SMP and OPT are platelet-like particles, but OPT ones resulted homogeneously and better disagglomerated within the polymeric matrix (Fig. 1), suggesting a good wettability and compatibility, with consequent enhanced mechanical behavior.

3.2. *Kinetic properties of protease immobilized on chitosan/clay nanocomposite films*

The addition of both nanoclays always affected the IY, resulting the amount of covalently bonded protein lower for all clay/CS membranes with respect to the clay-free carrier. Similar results have been reported by other authors [6], who proved that the addition of Na-bentonite into CS beads resulted in a lower immobilization yield for lipase. For both SMP and OPT composite systems, the percentage of immobilized proteins did not significantly change using different nanoclay

concentrations, as testified by the comparable IY values (18% for SMP-composite system and 14–17% for OPT-composite system).

The kinetic study, carried out on bromelain covalently immobilized on the novel produced clay/CS composite systems, allowed us to investigate the effect of carrier modification (due to the addition of high nano-clay concentrations) on the catalytic properties of the reference enzyme. All the kinetics followed the hyperbolic behavior described by the Michaelis–Menten equation (Fig. 8) and the catalytic properties of biocatalysts are reported in Table 2.

Despite clay/CS composite systems approximately linked the same amount of protein, significant differences were revealed in the catalytic performance of biocatalysts. Protease on SMP membranes showed V_{max} and K_M values similar to those observed for the clay-free biocatalyst (Table 2). Contrariwise, bromelain on OPT carriers showed the highest V_{max} and k_{cat}. These values were about 3-fold and 3.5-fold higher (respectively) in comparison to the clay-free enzyme as well as the SMP composite systems, thus suggesting a greater product release velocity. An increased V_{max} can be induced by conformational changes of biocatalysts, which can occur after the linkage to the support, as observed for other enzymes immobilized on clay/CS carriers, such as α-amylase and β-amylase [10]. However, bromelain on OPT composite systems showed a greater K_M (about 10-fold higher than the clay-free biocatalyst and about 6-fold higher with respect to the SMP biocatalysts), thus indicating a lower enzyme–substrate complex formation. An increase of K_M values can be caused by diffusion limitations or steric hindrance due to the clay mineral particles, as evidenced by other authors who immobilized enzymes on MMT or modified CS–clay supports [10,38,39]. Furthermore, for both SMP and OPT, the addition of various nanoclay amounts did not significantly affect either V_{max} or K_M.

Overall, the decrease of K_a revealed for all the biocatalysts on clay/CS membranes in comparison to the clay-free sample, indicated a lower apparent affinity of the protease for the synthetic substrate. These results could be ascribed to the increased rigidity of the carrier, which could limit the mobility of immobilized enzyme, as already proved [20]. Among the clay/CS biocatalysts, bromelain on SMP showed higher K_a values with respect to OPT composite systems. Comparing the two different nanoclay types, the greater apparent affinity of the protease for the synthetic substrate was revealed immobilizing bromelain on SMP-70 (K_a value 3.10 min^{-1} μM) or on OPT-70 (K_a value 1.78 min^{-1} μM).

4. Conclusions

Clay/CS composite systems, based on low amounts of chitosan, used as binder, and high amounts of nanoclays, were produced using two different kinds of montmorillonite, i.e. SMP (a high purity unmodified MMT) and Optigel (an activated MMT), in order to propose them as novel carriers for the covalent enzyme immobilization. Compact systems were obtained in all cases, characterized by a very uniform and homogeneous surface for OPT based composites and by several agglomerates and defects for SMP ones. The occurred electrostatic interaction between the chitosan NH_3^+ groups and the negatively charged sites of the clay was demonstrated by means of FTIR/ATR investigation. Decreased hydrogen bonds dissociation temperature and remarkably enhanced chitosan degradation temperature values were detected for the composite systems compared to the clay-free sample, demonstrating that the nanoclays are able to act as thermal barrier. Higher σ_{max} and Young modulus values were revealed in the case of OPT based composite systems with respect to the SMP based ones, due to OPT better distribution and interaction with the chitosan chains, as evident from the reported SEM micrographs.

Both SMP and OPT composite systems appeared to be suitable carriers for the covalent immobilization of bromelain and the addition of various nanoclay amounts did not affect neither the protein binding capacity nor the catalytic properties of the enzyme. Protease immobilized on OPT carriers showed the highest product release velocity, despite the fact that the apparent affinity was greater using SMP composite systems.

Conflicts of interest

The authors declare no conflict of interest.

Acknowledgement

This work was supported by BioEnBi project “Biotecnologie enzimatiche innovative per processi di chiarifica sostenibili nel settore birrario” (Grant 85-2017-15362), funded by Lazio Innova Spa, Lazio Region (Italy) in the context of Progetti Gruppi di Ricerca, Lazio Innova 2018–2020.

REFERENCES

[1] An N, Zhou CH, Zhuang XY, Tong DS, Yu WH. Immobilization of enzymes on clay minerals for biocatalysts and biosensors. Appl Clay Sci 2015;114:283–96.
[2] Sedaghat ME, Ghiaci M, Aghaei H, Soleimanian-Zad S. Enzyme immobilization. Part 4. Immobilization of alkaline phosphatase on Na-sepiolite and modified sepiolite. Appl Clay Sci 2009;46:131–5.
[3] Kaushal J, Seema, Singh G, Arya SK. Immobilization of catalase onto chitosan and chitosan–bentonite complex: a comparative study. Biotechnol Rep (Amst) 2018;18:e00258.
[4] Gopinath S, Sugunan S. Enzymes immobilized on montmorillonite K 10: effect of adsorption and grafting on the surface properties and the enzyme activity. Appl Clay Sci 2007;35:67–75.
[5] Mardani T, Khiabani MS, Mokarram RR, Hamishehkar H. Immobilization of α-amylase on chitosan–montmorillonite nanocomposite beads. Int J Biol Macromol 2018;120:354–60.
[6] Tu N, Shou J, Dong H, Huang J, Li Y. Improved catalytic performance of lipase supported on clay/chitosan composite beads. Catalysts 2017;7:302–14.
[7] Aydemir T, Güler S. Characterization and immobilization of *Trametes versicolor* laccase on magnetic chitosan–clay composite beads for phenol removal. Artif Cells Nanomed Biotechnol 2015;43:425–32.
[8] Andjelković U, Milutinović-Nikolić A, Jović-Jovičić N, Banković P, Bajt T, Mojović Z, et al. Efficient stabilization of *Saccharomyces cerevisiae* external invertase by immobilisation

on modified beidellite nanoclays. Food Chem 2015;168:262–9.
[9] Ding XL, Henrichs SM. Adsorption and desorption of proteins and polyamino acids by clay minerals and marine sediments. Mar Chem 2002;77:225–37.
[10] Chang MY, Juan RS. Activities, stabilities, and reaction kinetics of three free and chitosan–clay composite immobilized enzymes. Enzyme Microb Technol 2005;36:75–82.
[11] Chang MY, Juang RS. Use of chitosan–clay composite as immobilization support for improved activity and stability of β-glucosidase. Biochem Eng J 2007;35:93–8.
[12] Thakur G, Singh A, Singh I. Chitosan–montmorillonite polymer composites: formulation and evaluation of sustained release tablets of Aceclofenac. Sci Pharm 2016;84:603–17.
[13] Thakur G, Singh A, Singh I. Formulation and evaluation of transdermal composite films of chitosan–montmorillonite for the delivery of curcumin. Int J Pharm Investig 2018;6:23–31.
[14] Rhim JW, Park HM, Ha CS. Bio-nanocomposites for food packaging applications. Prog Polym Sci 2013;38:1629–52.
[15] Kotal M, Bhowmich AK. Polymer nanocomposites from modified clays: recent advances and challenges. Prog Polym Sci 2015;51:127–87.
[16] Rhim JW, Hong SI, Park HM, Ng PKW. Preparation and characterization of chitosan-based nanocomposite films with antimicrobial activity. J Agric Food Chem 2006;54:5814–22.
[17] Clapp CE, Emerson WW. Reactions between Ca-montmorillonite and polysaccharides. Soil Sci 1972;114:210–6.
[18] Wang SF, Chen L, Tong YJ. Structure–property relationship in chitosan-based biopolymer/montmorillonite nanocomposites. J Polym Sci Part A: Polym Chem 2006;44:686–96.
[19] Darder M, Colilla M, Ruiz-Hitzky E. Biopolymer–clay nanocomposites based on chitosan intercalated in montmorillonite. Chem Mater 2003;15:3774–80.
[20] Benucci I, Liburdi K, Cacciotti I, Lombardelli C, Zappino M, Nanni F, et al. Chitosan/clay nanocomposite films as supports for enzyme immobilization: an innovative green approach for winemaking applications. Food Hydrocoll 2018;74:124–31.
[21] Lu X, Hu J, Yao X, Wang Z, Li J. Composite system based on chitosan and room-temperature ionic liquid: direct electrochemistry and electrocatalysis of hemoglobin. Biomacromolecules 2006;7:975–80.
[22] Shi Q, Li Q, Shan D, Fan Q, Xue H. Biopolymer–clay nanoparticles composite system (chitosan–laponite) for electrochemical sensing based on glucose oxidase. Mater Sci Eng C 2008;28:1372–5.
[23] Zappino M, Cacciotti I, Benucci I, Nanni F, Liburdi K, Valentini F, et al. Bromelain immobilization on microbial and animal source chitosan films, plasticized with glycerol, for application in wine-like medium: microstructural, mechanical and catalytic characterisations. Food Hydrocoll 2015;45:41–7.
[24] Lieder R, Darai M, Örlygsson G, Sigurjonsson OE. Solution casting of chitosan membranes for in vitro evaluation of bioactivity. Biol Proced Online 2013;15:11–21.
[25] Aybastıera Ö, Demira C. Immobilization of *Candida antarctica* lipase A on chitosan beads for the production of fatty acid methyl ester from waste frying oil. Energ Sources Part A 2014;36:2313–9.
[26] Bradford MM. A rapid and sensitive method for the quantification of microgram quantities of protein utilizing the principle of protein-dye binging. Anal Biochem 1976;72:248–54.
[27] Hale LP, Greer PK, Trinh CT, James CL. Proteinase activity and stability of natural bromelain preparations. Int Immunophacol 2005;5:783–93.
[28] Chen SC, Wu YC, Mi FL, Lin YH, Yu LC, Sung HW. A novel pH-sensitive hydrogel composed of N O-carboxymethyl chitosan and alginate cross-linked by genipin for protein drug delivery. J Control Release 2004;96:285–90.
[29] Awad WH, Gilman JW, Nyden M, Harris RH Jr, Sutto TE, Callahan J, et al. Thermal degradation studies of alkyl-imidazolium salts and their application in nanocomposites. Thermochim Acta 2004;9:3–11.
[30] Leite I, Soares A, Carvalho L, Raposo C, Malta O, Silva S. Characterization of pristine and purified organobentonites. J Therm Anal Calorim 2009;100:563–9.
[31] Silva SM, Braga CR, Fook MV, Raposo CM, Carvalho LH, Canedo EL. Application of infrared spectroscopy to analysis of chitosan/clay nanocomposites. In: Infrared spectroscopy – materials science, engineering and technology. InTech; 2012. p. 43–62.
[32] Han YS, Lee SH, Choi KH, Park I. Preparation and characterization of chitosan–clay nanocomposites with antimicrobial activity. J Phys Chem Solids 2010;71:464–7.
[33] Paluszkiewicz C, Stodolak E, Hasik M, Blazewicz M. FT-IR study of montmorillonite–chitosan nanocomposite materials. Spectrochim Acta Part A 2011;79:784–8.
[34] Chuang WY, Young TH, Yao CH, Chiu WY. Properties of the poly(vinyl alcohol)/chitosan blend and its effect on the culture of fibroblast in vitro. Biomaterials 1999;20:1479–87.
[35] Sakurai K, Maegawa T, Takahashi T. Glass transition temperature of chitosan and miscibility of chitosan/poly(N-vinyl pyrrolidone) blends. Polymer 2000;41:7051–6.
[36] Zeng M, Fang Z, Xu C. Effect of compatibility on the structure of the microporous membrane prepared by selective dissolution of chitosan/synthetic polymer blend membrane. J Membr Sci 2004;230:175–81.
[37] Garavand F, Rouhi M, Razavi SH, Cacciotti I, Mohammadi R. Improving the integrity of natural biopolymer films used in food packaging by crosslinking approach: a review. Int J Biol Macromol 2017;104:687–97.
[38] Sanjay G, Sugunan S. Glucoamylase immobilized on montmorillonite: synthesis, characterization and starch hydrolysis activity in a fixed bed reactor. Catal Commun 2005;6:525–30.
[39] Dinçer A, Becerik S, Aydemir T. Immobilization of tyrosinase on chitosan–clay composite beads. Int J Biol Macromol 2012;50:815–20.